

Erik Sahlée*, Ann-Sofi Smedman, Xiaoli Guo Larsén, Anna Rutgersson and Ulf Högström
Department of Earth Sciences, Uppsala University, Sweden

1. INTRODUCTION

Much effort during the last decades has been put into understanding the exchange of momentum, heat and moisture between the ocean and the atmosphere. But the last word concerning these processes is far from being said. Since direct measurements of these fluxes are difficult to make in the marine environment, a common approach is to relate them to more easily measured parameters as mean temperature gradients and wind speed through bulk coefficients. The main focus in this study is on the bulk transfer coefficients of sensible and latent heat e.g. the Stanton and Dalton number, C_H and C_E .

One effect that is under debate is the influence of sea spray from breaking waves on the heat fluxes. Andreas and DeCosmo (2002) reanalysed data from the HEXOS experiment and found that these effects starts to play a roll already at 10ms^{-1} . They also draw the conclusion that sea spray is responsible for 20-30% of the total flux in the wind speed range $15\text{-}18\text{ ms}^{-1}$. Larsén et al. (2004) found from measurements that the neutral Stanton number C_{HN} at 16 ms^{-1} was about 50% higher than predicted theoretically by surface renewal theory (Liu et al., 1979).

The main focus of this study is to see if and how sea spray is influencing the turbulent structure in the marine boundary layer. This is done by comparison of the cospectra for sensible and latent heat flux during different wind speeds.

2. THEORY

The turbulent fluxes of humidity and heat is often parameterised with the aid of the exchange coefficients according to the following relations:

$$\overline{w'q'} = C_E (U - U_0)(q_0 - q) \quad (1a)$$

$$\overline{w'\theta'} = C_H (U - U_0)(\theta_0 - \theta) \quad (1b)$$

where U and U_0 are the mean wind speeds (ms^{-1}), q and q_0 are the mixing ratios ($\text{kg}_{\text{H}_2\text{O}}\text{kg}_{\text{air}}^{-1}$) and θ and θ_0 are potential temperatures (K) each at a reference height (usually 10 m) and, index 0, at the sea surface. The sensible and latent heat fluxes (in Wm^{-2}) are then acquired through:

$$H = \rho C_p \overline{w'\theta'} \quad (2a)$$

$$\lambda_v E = \lambda_v \rho \overline{w'q'} \quad (2b)$$

where λ_v is the heat of evaporation (J kg^{-1}), ρ is the density of air (kg m^{-3}) and C_p is the specific heat at constant pressure ($\text{kg}^{-1}\text{K}^{-1}$).

In the literature one often discusses the neutral values of the transfer coefficients. The transformation of the C_H and C_E to their neutral counterparts, C_{HN} and C_{EN} , are made with the aid of Monin-Obukhov similarity theory and they take the form:

$$C_{EN} = \frac{k^2}{[\ln(z/z_0)][\ln(z/z_{0q})]} \quad (3a)$$

$$C_{HN} = \frac{k^2}{[\ln(z/z_0)][\ln(z/z_{0T})]} \quad (3b)$$

where k is the von Karmán constant, z_0 , z_{0T} and z_{0q} are the roughness lengths of

* Corresponding author address: Erik Sahlée, Uppsala University, Dept. of Earth Sciences, Meteorology, Villavägen 16, SE-752 36 Uppsala, Sweden; e-mail: Erik.Sahlee@met.uu.se

momentum, heat and humidity respectively. For these expressions to be correct, all the requirements for the Monin-Obukhov's similarity theory need to be fulfilled i.e. horizontal homogeneous surface, height constant fluxes and stationary conditions.

3. SITE AND MEASUREMENTS

3.1 The site

The measuring site, Östergarnsholm, is a small, flat island situated 4 km east of Gotland (Figure 1). The tower is situated at the south end of the island with its base just 1 m above the mean sea level. It has been running semi-continually since 1995. The actual sea level is constantly changing as a response of changing wind conditions. Since no measurement of the sea level is made in situ, the sea level has to be corrected with the aid of measurements of the sea level in Visby harbour.

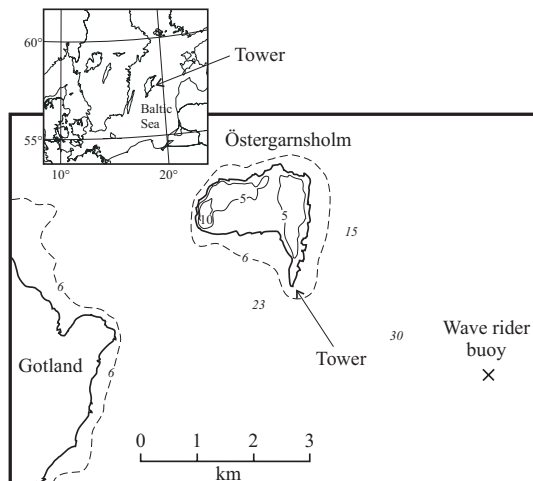


Figure 1. Map of the measuring site Östergarnsholm and its surroundings. The island is situated at 57°27'N, 18°59'E (from Johansson et al. 2003).

In Smedman et al., 1999 it was concluded that there isn't any serious influence of limited water depth on the turbulence structure in the surface layer. It was found that, for the 10 m level, 90% of the fluxes originated from 250 m beyond the shoreline and that during light-wind conditions, the phase speed of the dominating waves c_p varied between 92-99% of the deep-water value.

Wave data is gathered from a wave rider buoy, (run and owned by the Finnish Institute for Marine Research). The buoy is moored at 36 m depth, 4 km ESE of the island. Thus, the buoy is representing wave conditions for wind coming

from the south sector (80°-220°). In this direction the over water fetch is undisturbed for at least 150 km.

3.2 Tower measurement

The tower is equipped with slow response sensors for profile measurements of temperature, wind speed and wind direction. These sensors are placed at 7, 11.5, 14, 20 and 29 m above the tower base. Relative humidity is measured at 7m above the tower base.

Turbulent fluctuations are mainly recorded with SOLENT 101R2 (Gill Instrument, Lymington, UK) sonic anemometers placed at three levels (9, 16.5 and 25 m above the tower base). During certain periods, turbulence is measured with the MIUU turbulence instrument. This is a wind-vane mounted instrument with a hot-film sensor and additional platinum sensors for measurements of the temperature (dry- and wet-bulb).

Since November 2001, a LICOR-7500 open-path gas analyser is mounted on the tower at the lowest turbulence measuring level. This instrument gives the humidity and CO₂, both mean levels and turbulent fluctuations. Together with a Sonic anemometer the turbulent fluxes are calculated. The instrument has been running semi-continually since it was mounted.

3.3 Wave measurements

Wave data is recorded from the wave rider buoy at an hourly basis. Directional spectrum with 64 frequency bands is calculated from 1600s of data stored internally on the buoy.

The wave buoy also measures the bucket sea surface temperature at a depth of 0.5 m.

3.4 Data selection

The data used to investigate the turbulent humidity flux have been selected according to the following criteria:

- (i) Wind from the south sector (80°-220°)
- (ii) Wind speed at 10 m is greater than 2 ms⁻¹
- (iii) $|\theta_{10} - \theta_s|$ (Temperature difference between the sea surface and the air at 10 m) is larger than 1.0 K
- (iv) $|q_{10} - q_s|$ (The difference of mixing ratio between the sea surface and the air at 10 m) is greater than 10⁻⁴ kg_{H₂O}kg_{air}⁻¹.

- (v) The magnitude of the humidity flux $|\overline{w'q'}|$ is larger than $10^{-6} \text{ ms}^{-1} \text{ kg}_{\text{H}_2\text{O}}\text{kg}_{\text{air}}^{-1}$.
- (vi) Relative humidity less than 98%.
- (vii) Complete set of data for both the meteorological data and the wave data.

4. RESULTS

The total number of data points in this set is 385. All data are half hour averages.

Figure 2a shows the Dalton number C_E and Fig. 2b the neutral counterpart C_{EN} as a function of wind speed. C_E seems to be constant over the whole range of wind speeds but C_{EN} appears to slightly increase with increasing wind speed although with large spread during the higher wind speeds. The data taken from the MIUU instruments, although they are fewer, show less scatter than the data measured from the LICOR.

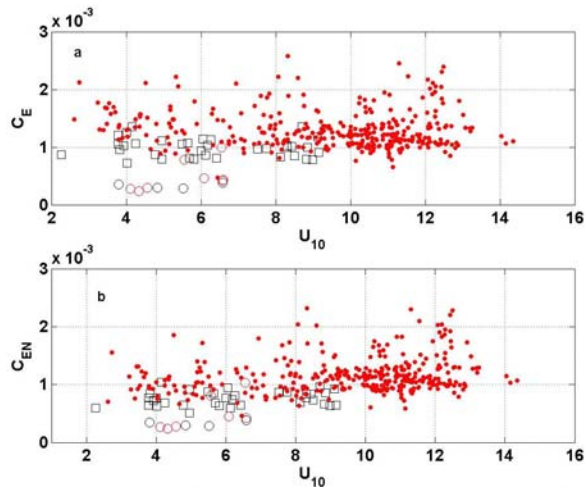


Figure 2. The Dalton number, C_E (a), and the neutral Dalton number, C_{EN} (b), as function of wind speed at 10 m. The colour red represents measurements with the LICOR and the black colour represents measurements made with the MIUU-instrument. Open circles represents stable conditions ($z/L > 0$).

Figure 3a and Figure 3b show the stability dependence of C_E and C_{EN} . Important features in these figures are:

1) The difference in the mean value of the exchange coefficient between unstable and stable stratification. The mean value of the unstable data for C_{EN} is $1.12 \cdot 10^{-3}$ which is in line with earlier studies (see for instance Large and Pond, 1982 and DeCosmo et al. 1996). The mean value for the few data in the stable group

is $0.43 \cdot 10^{-3}$. Other authors have noted the jump in C_{EN} before (for instance, Oost et al. 2000).

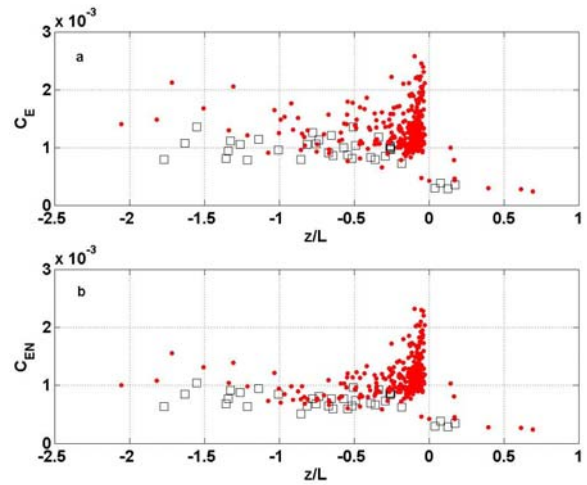


Figure 3. The Dalton number, C_E (a), and the neutral Dalton number, C_{EN} (b), as function of the stability parameter z/L . Dots represent measurements with the LICOR, open squares represent measurements with the MIUU instrument.

2) The large spread of the data points close to neutral stratification, from $0.9 \cdot 10^{-3}$ to $2.3 \cdot 10^{-3}$. Since the spread of the neutral Dalton number gets larger as $z/L \rightarrow 0$ the conclusion must be drawn that this “correction” of C_E to its neutral value, C_{EN} , isn’t properly made. Or to put it in another way: There are other parameters than stability that have an influence on the value of C_E .

To investigate this further, case studies were made. Since the aim of the study is to see if and how sea spray is influencing the turbulent structure, cases with increasing wind speed over a short time period were selected. Three cases were found where the wind direction was from the south sector.

The result concerning the exchange coefficients during these periods is in line with the more general results, that is, C_E is kept constant for the whole wind speed range but there is a tendency for C_{EN} to increase with increasing wind speed.

Cospectra for sensible and latent heat fluxes were calculated. An interesting behaviour of the cospectra for the cases where the wind is increasing is that a peak at a high frequency starts to emerge as the wind speed is increasing. This behaviour is seen in all three

cases that were selected. Figure 4 shows a typical example of the cospectra of wq at a low wind speed and Figure 5 shows a typical example of the cospectra at a higher wind speed (approximately 10 ms^{-1} and higher).

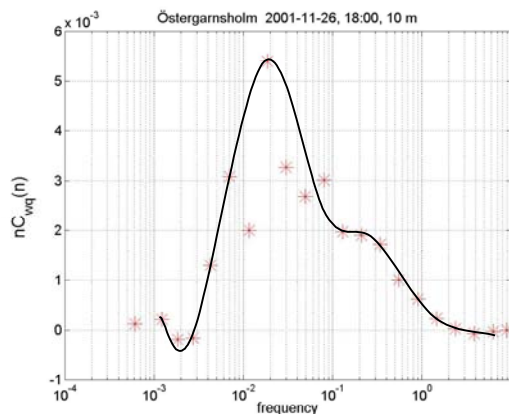


Figure 4. Typical example of a cospectrum of wq at low wind speed, with only one peak at a low frequency. Measurement from LICOR-7500 and a Sonic R2

The high frequency maximum starts to emerge approximately at a wind speed of 7 ms^{-1} or, in terms of significant wave height, roughly at 0.5 m. The frequency of the maximum is shifted slightly towards higher frequencies as the wind speed/wave height increases. Cospectra of wt show the same behaviour.

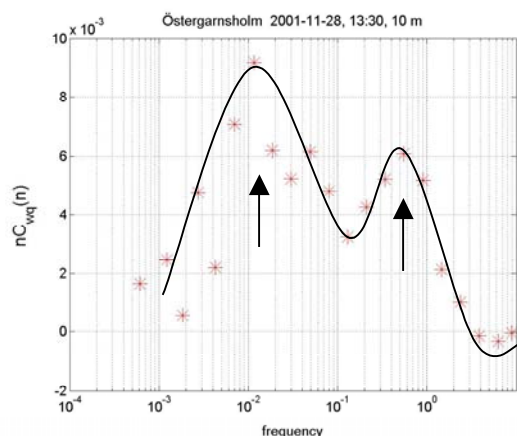


Figure 5. Typical example of a cospectrum at higher wind speed. The arrows points at the two maximums.

This 'double structure' of the wq -cospectra has been reported earlier, Schmitt et al. 1979 and Sempreviva and Gryning (1996) label it 'saddle-shape structure'. Phelps and Pond (1971)

observed double peaked temperature spectra from over sea measurements made from R/V Flip outside San Diego.

One way of investigating the relation of the high frequency peak and low frequency peak behaviour is to plot the ratio of the cospectral-levels of the two peaks against parameters that one suspects may have an influence on the ratio. This is done for both the $\overline{w'q'}$ and $\overline{w't'}$ cospectra in Figure 6.

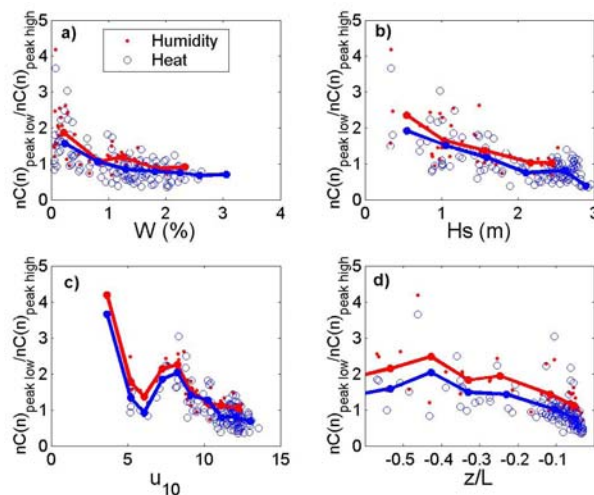


Figure 6. The ratio of the spectral levels of the low frequency peak and the high frequency peak plotted against **a)** Whitecap coverage in % (calculated with u -as suggested by Laon et al. (2004) **b)** Significant wave height **c)** Wind speed **d)** The stability parameter z/L Red dots represent data for the wq peak ratio, blue circles represent data for the wt peak ratio. Lines connect the bin-averaged points.

The figure indicates that the high frequency peak gets more dominating as the wind speed increases. But the best scaling parameter seems to be the significant wave height. Of course, these parameters are more or less representing the same effect, they are connected; Higher wind leads to higher waves, a greater fraction of whitecaps and it also leads to stability close to neutral.

The bin averages for both the $\overline{w'q'}$ spectral ratio and the $\overline{w't'}$ spectral ratio seem to follow each other quite well.

There are fewer data points representing the wq spectral ratio than there are data representing the wt spectral ratio.

How does this ratio affect the exchange coefficients? One way of illustrating how

complex the issue of the exchange coefficients is, is to make an area plot where C_H or C_E depends on *two* variables. This is done in Figure 7 where the spectral peak ratio is plotted against significant wave height and where the colored fields represent different values of C_H . A similar plot has been made for C_E (not shown) but the picture is clearer for the C_H plot since the amount of data is greater.

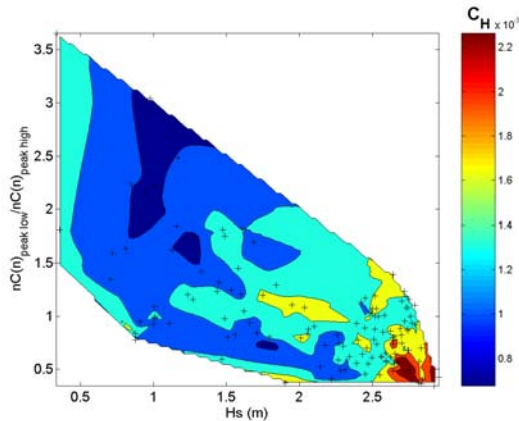


Figure 7. C_H as a function of the ratio of the cospectral peaks and the significant wave height.

The highest values of C_H is reached when the wave height is greater than 2.5 m and the ratio between the level of the high frequency peak and the low frequency peak is less than or equal to 0.5. For wave heights greater than 2.5 m the value of C_H can vary between 1.2 and 2.2 depending on the value of the peak ratio. A higher value of the ratio (i.e. a less dominating high frequency peak) gives a lower value of C_H and vice versa.

A comparison of the $\overline{w't'}$ cospectra between turbulence instruments at different levels on the tower has also been made. Generally, during low wind speed, in these cases, the $\overline{w't'}$ cospectra are similar at all levels as presented in Figure 8.

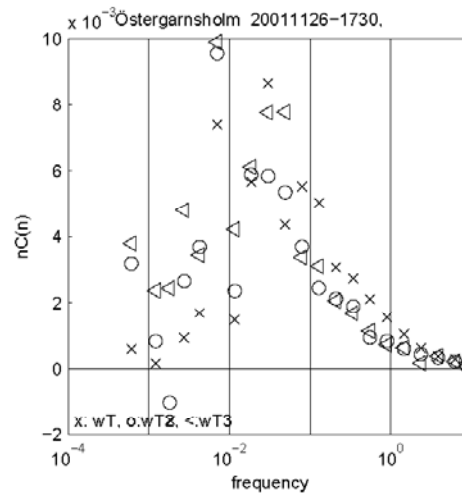


Figure 8, $\overline{w't'}$ cospectra at three levels in lin-log representation. Wind speed at 10m is 5 ms^{-1} . The different symbols represent the $\overline{w't'}$ cospectra at different heights, x – 9 m, open circles – 16 m and triangles 25 m above the tower base.

The picture looks completely different as the wind speed increases. Figure 9 shows an example of $\overline{w't'}$ cospectra a wind speed of approximately 12 ms^{-1} .

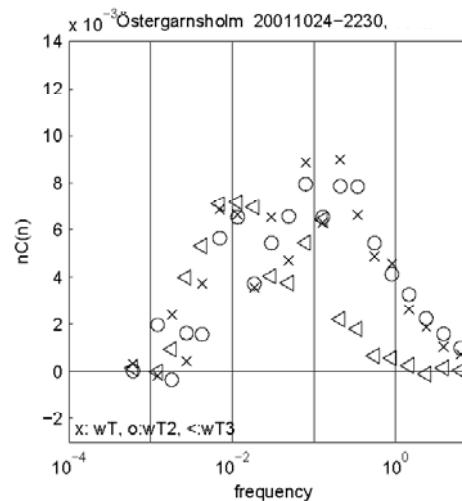


Figure 9, $\overline{w't'}$ cospectrum at three levels in lin-log representation. The wind speed at 10 m is 12 ms^{-1} . Symbols as in Figure 8.

At this occasion the high frequency peak can only be seen at the two lowest levels. At 25 m, there's only one clearly defined peak at a low

frequency. At some other occasions the high frequency peak can be seen at all three levels, although the level of the peak is highest at 9 m.

5. DISCUSSION

Earlier studies reporting the double structure, or saddle shape in temperature spectra all tried to explain the phenomenon as an effect of stability because the effect emerges close to neutrality. In this paper another approach is being made. The results presented above shows some evidence that support the theory that the high frequency maximum is induced from below by the wave field.

A secondary peak at a higher frequency start to emerge at wind speeds when the waves begin to break. The only way a breaking wave can influence the w_t and w_q cospectra is through sea spray. When the sea spray is evaporating it cools the air and supply water vapor, thus increasing the turbulent fluxes of sensible- and latent heat (Andreas and DeCosmo, 2002). This theory is supported by the fact that the secondary peak level increase as the wind speed and wave height increase. It is not to far fetched to assume that the higher a breaking wave is the more sea spray is produced.

Another piece of evidence supporting this theory is the height dependence of the high frequency maximum. The maximum is much less pronounced at the highest measuring level (if it exists at all) thus suggesting that the high frequency maximum is a result of processes close to the sea surface.

The low frequency peak represents the large-scale eddies that are present during unstable atmospheric conditions.

Studies of the temperature gradient during hurricane situations (Korolev et al. 1990, Cione et al. 2000) show that the temperature difference between the sea surface and the air increase as the wind speed increase. This effect is also seen in the profile measurements of the temperature at Östergarnsholm, although of course, the vertical extent of the affected layer is probably much less and the effect on the temperature seems to be a cooling of only about 0.1 K at the highest wind speed. This cooling, small though it may seem, could perhaps be enough to create a thin stably stratified layer close to the sea surface.

As seen in Figure 7, sea spray could also be one reason of the scatter of C_H (and C_E) when plotting these against just a single variable (usually wind speed at 10 m). This figure

indicates that the exchange coefficient never can be correctly parameterized with only one variable.

6. REFERENCES

Andreas, E. and DeCosmo, J. 2002: The signature of sea spray in the HEXOS turbulent heat flux data, *Boundary-Layer Meteorol.*, **103**, 303-333.

Cione, J. J., Black, P. G. and Houston, S.H., 2000: Surface Observations in the Hurricane Environment, *Mon. Wea. Rev.*, **128**, 1550-1561

Johansson, C. 2003: Influence of External Factors on the Turbulence Structure in the Boundary Layer, *PhD-Thesis*, Department of Earth Sciences, Meteorology, Uppsala University

Korolev, V. S., Petrichenko, S. A. and Pudov, V. D., 1990: Heat and moisture transport between the ocean and atmosphere in tropical storms Tess and Skip (English translation), *Sov. Meteor. Hydrol.*, **3**, 92-94

Lafon, C., Piazzola, J., Forget, P., Le Calve, O. and Despiau S., 2004: Analysis of the variation of the whitecap fraction as measured in a coastal zone, *Boundary-Layer Meteorol.*, **111**, 339-360

Large, W. G. and Pond, S. 1982: Sensible and latent heat flux measurements over the ocean, *J. Phys. Oceanogr.* **12**, 464-482.

Larsén, X. G., Smedman, A. and Högström, U., 2004: Air-sea exchange of sensible heat over the Baltic Sea, *Q. J. R. Meteorol. Soc.*, **130**, 519-539

Liu, W. T., Katsaros, K. B. and Businger, J. A., 1979: Bulk parameterization of air-sea exchanges of heat and water vapor including the molecular constraints at the interface, *J. Atmos. Sci.*, **36**, 1722-1735

Oost, W. A., Jacobs, C. M. J. and van Oort C., 2000: Stability effects on heat and moisture fluxes at sea, *Boundary-Layer Meteorol.* **95**, 271-302.

Phelps, G. T., and Pond S., 1971: Spectra of the temperature and humidity fluctuations of the fluxes of moisture and sensible heat in the marine boundary layer, *J. Atmos. Sci.*, **28**, 918-928

Schmitt, K. F., Friehe, C. A. and Gibson, C. H. 1979: Structure of Marine Surface Layer Turbulence, *J. Atmos. Sci.*, **36**, 602-618

Sempreviva A. M. and Gryning, S-E., 1996: Humidity fluctuations in the marine boundary layer measured at a coastal site with an infrared humidity sensor.

Smedman, A., Högström, U., Bergström, H., Rutgersson, A., Kahma, K. K. and Pettersson, H., 1999: A case study of air-sea interaction during swell conditions, *J. Geophys. Res.*, **104**, 25, 833-25,851